Analysis of the role of mobility-lifetime products in the performance of amorphous silicon *p-i-n* solar cells

J. M. Asensi,[a] J. Merten, C. Voz, and J. Andreu
Departament de Física Aplicada i Optica, Universitat de Barcelona, Avinguda Diagonal 647, Planta 4, E-08028 Barcelona, Spain

(Received 13 October 1998; accepted for publication 30 November 1998)

An analytical model of an amorphous silicon *p-i-n* solar cell is presented to describe its photovoltaic behavior under short-circuit conditions. It has been developed from the analysis of numerical simulation results. These results reproduce the experimental illumination dependence of short-circuit resistance, which is the reciprocal slope of the $I(V)$ curve at the short-circuit point. The recombination rate profiles show that recombination in the regions of charged defects near the *p-i* and *i-n* interfaces should not be overlooked. Based on the interpretation of the numerical solutions, we deduce analytical expressions for the recombination current and short-circuit resistance. These expressions are given as a function of an *effective* $\mu\tau$ product, which depends on the intensity of illumination. We also study the effect of surface recombination with simple expressions that describe its influence on current loss and short-circuit resistance. © *1999 American Institute of Physics.* [S0021-8979(99)03705-6]

I. INTRODUCTION

The collection mechanism in *a*-Si:H-based *p-i-n* solar cells can be studied theoretically by means of numerical[1–3] and analytical models[4,5]. Numerical treatments using computer calculation have often been preferred due to the difficulty of solving the fundamental formulas for analysis (Poisson and continuity equations). However, the interpretation of the experimental behavior of the cell from numerical results is often complicated by the large number of parameters involved. Furthermore, many of the material parameters required are experimentally inaccessible or imperfectly known. Analytical models have the drawback of requiring strong assumptions in order to solve the transport equations, but the simplicity of their solutions allows a straightforward link with the experimental results.

There have been fewer fully analytical attempts to describe the collection mechanism in *a*-Si:H *p-i-n* solar cells than numerical treatments. The main attempt is probably the uniform-field model of Crandall,[4] whose main assumptions are: constant electric field, negligible diffusion in the *i* layer, and the use of the Shockley–Read–Hall expression for recombination as derived for a two-state recombination center. These assumptions lead to a very simple expression for the photocurrent as a function of the two carrier drift lengths. Later, Hubin and Shah[5] proposed a variation of Crandall's model, in which a more realistic description of recombination in *a*-Si:H is introduced. They consider the amphoteric nature of the dangling bond, the main recombination center in *a*-Si:H, and use a recombination function based on a single type of three-state recombination center. In this way, they explain some of the differences between Crandall's analytical results and the more realistic models based on numerical simulation:[1] for example, this treatment shows that it is the carrier with the shorter drift length that will determine collection.

Recently, we used the uniform-field model of Hubin and Shah to interpret the variable illumination measurement of the short-circuit resistance R_{sc} of *a*-Si:H *p-i-n* solar cells:[6] i.e., the reciprocal slope $(\delta V/\delta I)_{V=0}$ of the $I(V)$ curve at the short-circuit point. Over a wide range of illumination levels, R_{sc} is inversely proportional to the short-circuit current I_{sc}. In this situation, the R_{sc} value is related to the voltage-dependent photocurrent collection and can be calculated by the uniform-field theory. Thus, if R_{sc} is plotted as a function of I_{sc}, it is possible to extract the value of an *effective* $\mu\tau$ product which suitably combines the $\mu\tau$ products of electrons and holes in the layer (more recently, other authors[7] reported a study which is similar but based on the Crandall theory).

Although the method is straightforward and has been satisfactorily applied as a quantifying tool for the state of degradation of *a*-Si:H solar cells and modules,[6] some experimental results question the validity of the uniform-field model used to interpret variable illumination measurements:

(a) In general, the $\mu\tau_{eff}$ value deduced from R_{sc} applying the uniform-field model is significantly lower (by up to 1 order of magnitude) than the one obtained from photoconductivity in intrinsic material.

(b) The R_{sc} dependence on illumination level is quasilineal: in most samples $R_{sc} \propto I_{sc}^{\gamma}$ where $\gamma < 1$ is found. In fact, if the value of $\mu\tau_{eff}$, deduced applying the uniform-field model [see Eq. (10) in Sec. II) is plotted as a function of I_{sc}, $\mu\tau_{eff}$ increases as the illumination level increases (see Fig. 1).

In this article, numerical simulation is used to show that these effects could be correlated with the charged defect states which necessarily exist near the *p-i* and *i-n* interfaces. For low and intermediate illumination levels, most of the recombination occurs in these regions. When illumination is

[a]Electronic mail: jmasensi@electra.fao.ub.es

 © 1999 American Institute of Physics

Downloaded 15 Jun 2010 to 161.116.168.169. Redistribution subject to AIP license or copyright; see http://jap.aip.org/jap/copyright.jsp

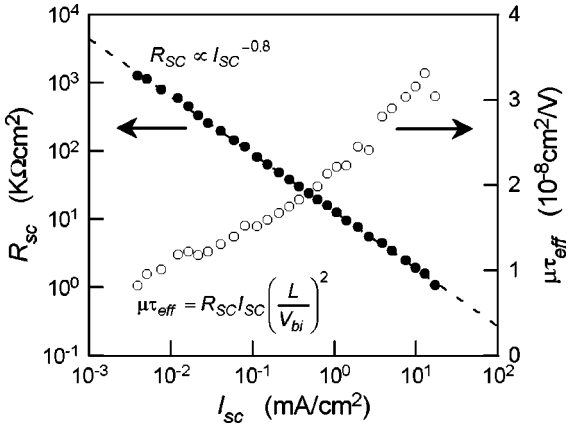

FIG. 1. Variable irradiance measurement of R_{sc} in *a*-Si:H *p-i-n* solar cells. The value of $\mu\tau_{eff}$ deduced from Eq. (10) (uniform-field model) is shown.

increased (for $I_{sc} > 10$ mA/cm^2), the charged defects are neutralized and the importance of the recombination near the interfaces decreases. Only in this case of high illumination are the uniform-field model assumptions valid. From the numerical results we develop a more detailed analytical description of collection in *p-i-n a*-Si:H solar cells. Our description includes the prominent role of charged defects in the *i* layer and enables a more general $\mu\tau_{\rm eff}$ depending on light intensity to be defined.

The paper is organized as follows. In Sec. II, we review the assumptions of the uniform-field model of Shah and Hubin, and show the expression deduced for short-circuit resistance R_{sc} as a function of the standard *effective* $\mu\tau$ product. In Sec. III, we describe our numerical model and present the full set of equations used in the computer simulation. Our numerical treatment was simplified for a better comparison with the results of the uniform-field model description. We then simulate a variable illumination measurement of R_{sc} and show that recombination in the charged regions at interfaces is not negligible. In Sec. IV we present the analytical description of the *p-i-n* solar cell including the effect of the charged regions. We show that, in thermodynamic equilibrium, the electric field profile, and the widths of the charged regions near the *p-i* and *i-n* interfaces can be deduced employing dangling bond statistics. In particular, we show that the use of the ''thin solar cell'' approach leads to straightforward expressions. We then study the effect of illumination on the electric field, carrier density, and recombination profiles. From this analysis the recombination current and the short-circuit resistance can be given as a function of a new effective $\mu\tau$ product which adequately combines the effect of the different regions on the *i* layer. Section IV closes with an analysis of the influence of surface recombination.

II. UNIFORM-FIELD MODEL AND $\mu\tau$ PRODUCT

Hubin and Shah[5] solved the problem of bulk collection in a *p-i-n* solar cell under these three basic assumptions:

(a) constant electric field in the *i* layer,

(b) negligible diffusion in the *i* layer,

(c) bulk recombination in the *i* layer is determined by the neutral dangling bonds.

The two first assumptions are indeed applicable to thin *p-i-n* cells under small or negative voltage bias. These are the same restrictive assumptions as in Crandall's model. To deal with recombination by neutral dangling bonds, they introduce a linear approximation for the recombination function associated with a single type of recombination center that can exist in three charge states:[8]

$$R_{\rm DB} = \frac{n}{\tau_n^0} + \frac{p}{\tau_p^0}, \tag{1}$$

where n and p are the densities of free carriers (electrons and holes) and τ_n^0 and τ_p^0 are the capture times of free electrons and free holes, respectively, by neutral dangling bonds. The capture times are defined by

$$\tau_n^0 = (v_{\rm th}\sigma_n^0 N_{\rm DB})^{-1} \quad \text{and} \quad \tau_p^0 = (v_{\rm th}\sigma_p^0 N_{\rm DB})^{-1}, \tag{2}$$

where σ_n^0 and σ_p^0 are the capture cross sections of the free carriers by the neutral dangling bonds, $N_{\rm DB}$ is the total density of dangling bonds, and $v_{\rm th}$ is the thermal velocity.

Now, assuming a uniform generation rate G due to weakly absorbed light, the steady-state continuity and transport equations with the appropriate boundary conditions can be solved and the densities of free carriers as a function of the position x in the *i* layer can be obtained. On introducing $n(x)$ and $p(x)$ into Eq. (1), the total recombination in the *i* layer can be calculated, and from this the bulk collection χ (i.e., the fraction of the collected photocurrent divided by the total generation current in the *i* layer). Hubin and Shah found

$$\chi = \frac{1}{L}\frac{l_n l_p}{l_n \exp(L/L_C) - l_p \exp(-L/L_C)} \times \left[\exp\left(\frac{L}{L_C}\right) - \exp\left(-\frac{L}{L_C}\right)\right], \tag{3}$$

where L is the thickness of the *i* layer and L_C is the *collection length*:

$$L_C = 2\frac{l_n l_p}{l_n - l_p}, \tag{4}$$

where l_n and l_p are the drift lengths for free electrons and free holes. These lengths depend on the electric field in the *i* layer (E_i), the band mobilities for free carriers (μ_n and μ_p), and the capture times of free carriers by neutral dangling bonds (τ_n^0 and τ_p^0):

$$l_n = \mu_n \tau_n^0 |E_i| \quad \text{and} \quad l_p = \mu_p \tau_p^0 |E_i|. \tag{5}$$

In the case of a thin *p-i-n* device, the electric field strength is strong enough for the drift lengths to be much larger than the *i* layer thickness. Then Eq. (3) becomes

Downloaded 15 Jun 2010 to 161.116.168.169. Redistribution subject to AIP license or copyright; see http://jap.aip.org/jap/copyright.jsp

$$\chi = \frac{L_C^*}{L_C^* + L}, \tag{6}$$

where L_C^* is a *redefinition* of the collection length as

$$L_C^* = 2\frac{l_n l_p}{l_n + l_p} = \mu\tau_{\text{eff}}|E_i|, \tag{7}$$

where $\mu\tau_{\text{eff}}$ is an effective $\mu\tau$ product which suitably combines $\mu\tau$ products of electrons and holes:

$$\mu\tau_{\text{eff}} = 2\frac{\mu_n\tau_n^0 \cdot \mu_p\tau_p^0}{\mu_n\tau_n^0 + \mu_p\tau_p^0}. \tag{8}$$

It can be shown that if $l_n \approx l_p$ then Eq. (6) is also valid in the more general situation, i.e., when the drift lengths l_n and l_p are comparable to or shorter than the *i* layer thickness (see Ref. 5). Note that in this case $L_C^* \approx l_n \approx l_p$.

In accordance with Eq. (6) the loss current I_{rec} in the *i* layer can be expressed as

$$I_{\text{rec}} = \frac{L}{L_C^*} I_{\text{ph}} = \frac{L^2}{\mu\tau_{\text{eff}}(V_{\text{bi}} - V)} I_{\text{ph}}, \tag{9}$$

where I_{ph} is the generation current in the *i* layer ($I_{\text{ph}} = qGL$), V_{bi} is the built-in voltage, and V is the applied voltage.

In the short-circuit region, and neglecting the effect of ''parasite'' resistance (see Ref. 6), the slope of the $I(V)$ curve is determined by the voltage dependence of I_{rec}. Thus, differentiating Eq. (9) with respect to the applied voltage, the short-circuit resistance can be deduced:

$$R_{\text{sc}} \approx \left(\frac{dV}{dI_{\text{rec}}}\right)_{V=0} = \mu\tau_{\text{eff}}\left(\frac{V_{\text{bi}}}{L}\right)^2 I_{\text{sc}}^{-1}, \tag{10}$$

where the generation current I_{ph} is approximated to the short-circuit current I_{sc} (note that we assume $\chi \approx 1$). So if we plot R_{sc} as a function of I_{sc} it is possible to extract, from the region where R_{sc} is inversely proportional to I_{sc}, the value of $\mu\tau_{\text{eff}}$.

III. NUMERICAL SIMULATION

A. Simplifying assumptions

All numerical calculations in this article were carried out using the simulation model which was previously developed by our group.[3] Our computer program uses finite differences and the Newton technique to solve Poisson's equation and continuity equations for the complete diode. The flexibility of the program allows different model assumptions to be analyzed. Our aim here is to study the validity of the hypotheses of the uniform-field model [assumptions (a), (b) and (c), in Sec. II] that lead to Eqs. (9) and (10) for the recombination current and short-circuit resistance, respectively. Therefore, as an excessively detailed description of the diode could complicate the analysis, some simplifying assumptions were incorporated into the numerical treatment:

(a) The transport equations were solved only within the intrinsic layer, and boundary conditions were defined at the doped-layer/intrinsic-layer interfaces (*p*-*i* and *i*-*n*). This assumption reduces significantly the number of physical parameters involved: as will be shown later, the doped-layer influence is completely described by only five *i* layer boundary condition parameters.

(b) To find the trapped charge density and the recombination rate, only the dangling bonds were examined. This is a good assumption for the middle of the *i* layer, but is inadequate for the regions near the interfaces *p*-*i* and *i*-*n*, where the Fermi level significantly enters the tail states. However, the tail states mainly affect the trapped charge near the interfaces and are thought to create only a small distortion in the magnitude of the electric field. A similar effect is produced by the fixed space charge at the interfaces in the doped layers. In fact, these two effects can be included as a reduction of the built-in potential V_{bi}, one of the boundary conditions of the problem.

(c) The defect distribution throughout the *i* layer was assumed uniform and constant. This is the standard model of the density of states in *a*-Si:H (and a normal assumption for all uniform-field models). A further simplification is to assume that the defect states in the gap are discrete.

B. Model equations

The equations that must be solved numerically are Poisson's equation:

$$\frac{dE}{dx} = \frac{q}{\varepsilon}[(p - n) + Q(p,n)], \tag{11}$$

relating the derivative of the electric field E to the local charge (free electrons n, free holes p, and trapped charge Q); the current density equations, combining the two driving forces of carrier movement, drift and diffusion, with the total hole (j_p) and electron (j_n) currents:

$$j_p(x) = q\mu_p p(x)E(x) - kT\mu_p\frac{dp(x)}{dx}, \tag{12a}$$

$$j_n(x) = q\mu_n n(x)E(x) + kT\mu_n\frac{dn(x)}{dx}, \tag{12b}$$

and the two continuity equations:

$$\frac{dj_p(x)}{dx} = q[G - R(p,n)], \tag{13a}$$

$$\frac{dj_n(x)}{dx} = -q[G - R(p,n)], \tag{13b}$$

where G is the generation rate and $R(p,n)$ is the recombination rate.

As stated, we assume that the trapped charge and the recombination are only determined by dangling bonds. Thus, the trapped charge Q is

$$Q = [f^+(p,n) - f^-(p,n)]N_{\text{DB}}, \tag{14}$$

where N_{DB} is the constant density of dangling bonds in the *i* layer and f^+ and f^- are the occupation of the positive and negative dangling-bond states:[2]

Downloaded 15 Jun 2010 to 161.116.168.169. Redistribution subject to AIP license or copyright; see http://jap.aip.org/jap/copyright.jsp

$$f^+(p,n)=\frac{T^+(p,n)}{1+T^+(p,n)+T^-(p,n)}, \tag{15a}$$

$$f^-(p,n)=\frac{T^-(p,n)}{1+T^+(p,n)+T^-(p,n)}, \tag{15b}$$

with

$$T^+(p,n)=\frac{\sigma_p^0 p+\frac{1}{2}\sigma_n^+ N_C e^{-(E_C-E^+)/kT}}{\sigma_n^+ n+2\sigma_p^0 N_V e^{-(E^+-E_V)/kT}}, \tag{16a}$$

$$T^-(p,n)=\frac{\sigma_n^0 n+\frac{1}{2}\sigma_p^- N_V e^{-(E^--E_V)/kT}}{\sigma_p^- p+2\sigma_n^0 N_C e^{-(E_C-E^-)/kT}}, \tag{16b}$$

where σ_n^0 and σ_p^0 are the capture cross sections of electrons and holes by neutral dangling bonds, σ_n^+ is the capture cross section of electrons by positive dangling bonds, σ_p^- is the capture cross section of holes by negative dangling bonds, and E^+ and E^- are the effective energy levels of the $D^+ \leftrightarrow D^0$ and $D^- \leftrightarrow D^0$ transitions.

The rate of recombination via dangling bonds is given by

$$R=v_{\text{th}}(pn-n_i^2)\left(\frac{\sigma_n^+\sigma_p^0}{\sigma_n^+ n+2\sigma_p^0 N_V e^{-(E^+-E_V)/kT}}+\frac{\sigma_p^-\sigma_n^0}{\sigma_p^- n+2\sigma_n^0 N_C e^{-(E_C-E^-)/kT}}\right) f^0(p,n)N_{\text{DB}}, \tag{17}$$

where n_i is the equilibrium intrinsic concentration and f^0 is the occupation of the neutral dangling bonds:

$$f^0(p,n)=\frac{1}{1+T^+(p,n)+T^-(p,n)}. \tag{18}$$

Finally, this set of coupled differential equations must be solved with the appropriate boundary conditions. As stated above, these conditions are defined at the interfaces *p-i* and *i-n*. The first boundary condition refers to the potential difference across the *i* layer:

$$V(L)-V(0)=V_{\text{bi}}-V_{\text{ext}}, \tag{19}$$

where V_{bi} is the built-in potential, i.e., the difference in the electrostatic potential between the *p* layer and the *n* layer in equilibrium, and V_{ext} is the applied voltage. Note that the full built-in voltage is assumed to be applied over the *i* layer alone, and that the part of the potential lost in the doped layer space-charge regions is neglected.

The remaining boundary conditions define the current densities at the interfaces by effective surface-recombination velocities *S* for both holes and electrons. However, some simplification is possible: e.g., for majority carriers we can assume that the interfaces behave as ohmic contacts, and the corresponding *S* values are very high. Therefore, we can assume a constant majority-carrier concentration that is independent of the current density:

TABLE I. Values of parameters used for numerical calculations.

Principal intrinsic material parameters	
Band gap E_g (eV)	1.77
Effective densities of states N_C and N_V (cm^{-3})	4×10^{19}
Electron mobility μ_n ($\text{cm}^2/\text{V/s}$)	10
Hole mobility μ_p ($\text{cm}^2/\text{V/s}$)	4
Dangling bond density N_{DB} (cm^{-3})	10^{16}
Energy level of the $D^+ \leftrightarrow D^0$ transition E^+-E_V (eV)	0.735
Effective correlation energy U_{eff} (eV)	0.3
Capture cross-section of electrons by $D^0\sigma_n^0$ (cm^2)	5×10^{-16}
Capture cross-section of electrons by $D^+\sigma_n^+$ (cm^2)	2.5×10^{-14}
Capture cross-section of holes by $D^0\sigma_p^0$ (cm^2)	10^{-16}
Capture cross-section of holes by $D^-\sigma_p^-$ (cm^2)	5×10^{-15}
Capture times of free carriers by dangling bonds	
Capture time of electrons by $D^0\tau_n^0=(v_{\text{th}}\sigma_n^0 N_{\text{DB}})^{-1}$ (s)	2×10^{-8}
Capture time of electrons by $D^+\tau_n^+=(v_{\text{th}}\sigma_n^+ N_{\text{DB}})^{-1}$ (s)	4×10^{-10}
Capture time of holes by $D^0\tau_p^0=(v_{\text{th}}\sigma_p^0 N_{\text{DB}})^{-1}$(s)	10^{-7}
Capture time of holes by $D^-\tau_p^-=(v_{\text{th}}\sigma_p^- N_{\text{DB}})^{-1}$ (s)	2×10^{-9}
Doped material parameters	
Fermi-level in the *p*-layer E_F-E_V (eV)	0.58
Fermi-level in the *n*-layer E_C-E_F (eV)	0.58
Interface recombination velocity of minority carriers S_L and S_0 (cm/s)	10

$$p(0)=p_{\text{eq}}(0) \quad \text{and} \quad n(L)=n_{\text{eq}}(L), \tag{20}$$

where $p_{\text{eq}}(0)$ and $n_{\text{eq}}(L)$ are the equilibrium hole and electron densities in the doped layers. For the minority-carrier currents [$j_p(L)$ and $j_n(0)$] we use the more general form:

$$j_p(L)=qS_L[p(L)-p_{\text{eq}}(L)], \tag{21a}$$

$$j_n(0)=qS_0[n(0)-n_{\text{eq}}(0)], \tag{21b}$$

where $p_{\text{eq}}(L)$ and $n_{\text{eq}}(0)$ are the equilibrium minority-carrier densities in the doped layers, and S_L and S_0 are the interface recombination velocities for the minority carriers at the interfaces. Note that the currents given by Eq. (21) are loss currents. The case $S_L=S_0=0$ is an ideal situation where the interfaces are perfectly blocking contacts for the minority carriers.

C. Simulation results

Variable irradiance measurement of R_{sc} over a range of illumination levels from 10^{-5} to 10^2 mA/cm^2 (for I_{sc}) was simulated. It was considered uniform-light illumination. The device simulated was a 0.3-μm-thick *a*-Si:H solar cell. Model parameters are listed in Table I. These parameters are the typical ones for *a*-Si:H material in the annealed state (e.g., see Ref. 9): with these parameters and using Eq. (8) we obtain a $\mu\tau_{\text{eff}}$ value of 2.7×10^{-7} cm^2/V, and applying Eq. (7) we find 62 μm for the collection length L_C^* (note that this is much longer than the *i* layer thickness L).

Figure 2 shows the calculated short-circuit resistance R_{sc} and the $\mu\tau_{\text{eff}}$, deduced from R_{sc} by applying Eq. (10) as a function of the short-circuit current I_{sc}. At the lowest illu-

Downloaded 15 Jun 2010 to 161.116.168.169. Redistribution subject to AIP license or copyright; see http://jap.aip.org/jap/copyright.jsp

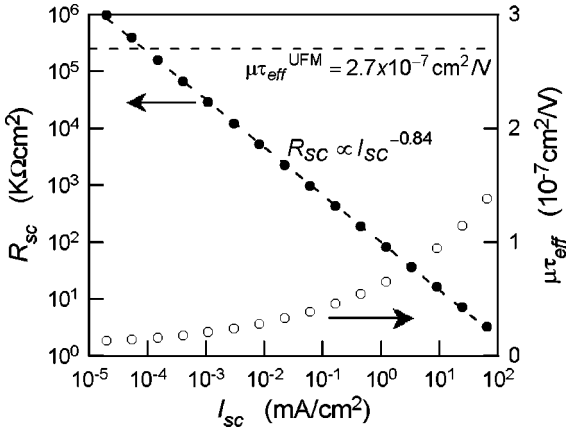

FIG. 2. Simulated short-circuit resistance R_{sc} as a function of the short-circuit current I_{sc}. The value of $\mu\tau_{eff}$ deduced from R_{sc} by applying Eq. (10) and the theoretical value of $\mu\tau_{eff}$ deduced from (8) (dashed line) are shown.

mination levels we find a value of $\mu\tau_{eff}$ approximately one order of magnitude smaller that predicted by the uniform-field theory. On the illumination level increasing, this difference decreases and the $\mu\tau_{eff}$ is close to the value theoretically predicted. In fact, one can see from Fig. 2 that the R_{sc} dependence on illumination is quasilineal: we find $R_{sc} \propto I_{sc}^{\gamma}$ with $\gamma = 0.84$. These results are consistent with the experimental data (see Fig. 1). Consequently, a detailed analysis of our simulation results is expected to reveal aspects of the physics of the device that are not included in the conventional uniform-field model.

Figure 3 shows some calculated profiles (density of trapped charge, electric field, and recombination rate) at short-circuit conditions for two different levels of illumination. The most important differences between simulation and the uniform-field model suppositions appear in the low-illumination regime (solid line in Fig. 3). In this regime, neutrality is only maintained in a small region within the *i* layer. In the regions near to the doped zones, dangling bonds are charged [Fig. 3(A)], altering the electric field [Fig. 3(B)] and clearly the recombination profile [Fig. 3(C)] . It can be observed that, in this case of low illumination, most of the recombination occurs close to the interfaces where the defects are in the charged state. So the collection, and probably its dependence on the applied voltage, must be controlled by these regions. When illumination increases, the neutral region increases and the charged regions shrink (dashed line in Fig. 3). The field inside the bulk of the *i* layer grows and the relative weight of the recombination through charged dangling bonds becomes much lower: note that only in the regime of very high illumination ($I_{sc} > 10^2$ mA/cm^2) could hypotheses (a) and (c) of the uniform-field model be considered valid.

Now we shift our attention to hypothesis (b) of the uniform-field model, i.e., that photocarrier transport occurs by field-assisted drift. Figure 4 shows the drift and the diffusion components of the hole current density under short-circuit conditions for the two cases of illumination. It can be seen that near the *p-i* interface, where holes are the majority carriers, both drift and diffusion contribute to the photocurrent. Therefore, diffusion cannot be overlooked when solving the hole transport equations in this region. As can also be seen, this effect decreases under very intense illumination and, only in this case, hypothesis (b) of the uniform-field model could be applied in the whole bulk of the *i* layer. To demonstrate more clearly that diffusion must be included for majority carriers close to the interfaces, in Fig. 5 we compare the profile of photogenerated hole density with the profile deduced from the uniform-field theory which overlooks diffusion [see Eq. (31) in Sec. IV C]. It can be seen that, at low

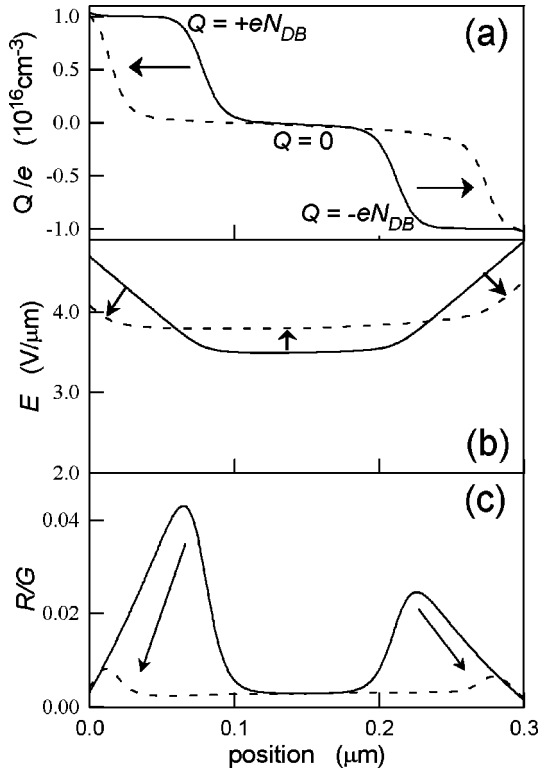

FIG. 3. Simulated profiles of (A) density of trapped charge, (B) electric field, and (C) recombination rate normalized to generation, at short-circuit conditions and for two illumination levels: low (solid line, $I_{sc} = 10^{-3}$ mA/cm^2) and high (dashed line, $I_{sc} = 10^2$ mA/cm^2). The arrows indicate evolution with illumination.

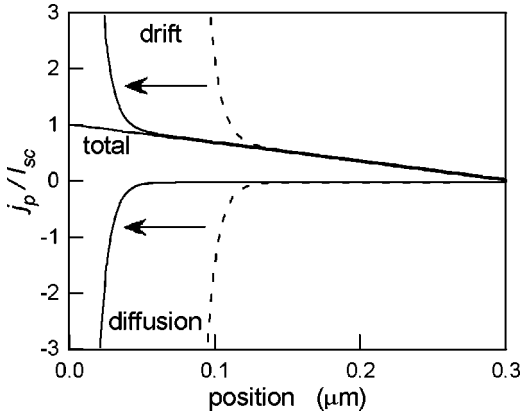

FIG. 4. Simulated profiles of the hole current density normalized to the total short-circuit current in the same conditions as in Fig. 3. The drift and the diffusion components of the current and the effect of the illumination level are shown.

Downloaded 15 Jun 2010 to 161.116.168.169. Redistribution subject to AIP license or copyright; see http://jap.aip.org/jap/copyright.jsp

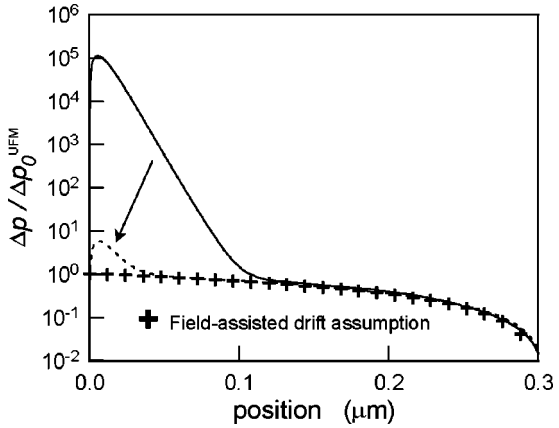

FIG. 5. Photogenerated hole profiles in the same conditions as in Fig. 3. Showing simulated profiles for the two illumination levels, and the theoretical profile obtained by neglecting both diffusion and recombination: $\Delta p(x)=\Delta p_0^{\mathrm{UFM}}(L-x)$ with $\Delta p_0^{\mathrm{UFM}}=(G\cdot L)/(\mu_p\cdot V_{\mathrm{bi}})$.

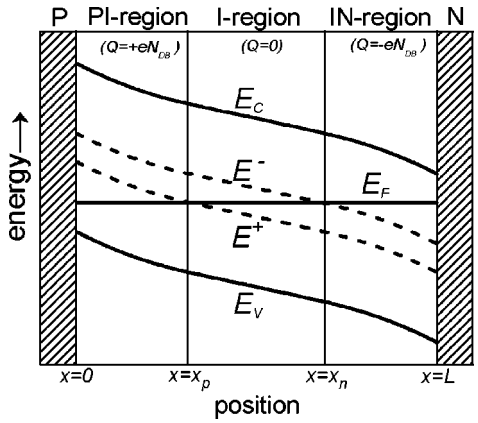

FIG. 6. Schematic energy band diagram of *a*-Si:H *p-i-n* solar cell in equilibrium.

illumination, the simulated photohole density at the *p-i* interface is significantly different from the theoretical value. As will be discussed later, the majority-carrier densities photogenerated near the interfaces are very sensitive to perturbations in the electric field (which could be due to illumination and/or voltage bias). Although this is not significant in calculating the loss of carrier collection, since recombination in these regions is determined by minority carriers, the complete description of the *p-i-n* diode must take into account the effect of the majority carriers injected from the *p-i* and *i-n* contacts.

In summary, numerical simulation has demonstrated that hypotheses used in the uniform-field model are not fulfilled, especially at low illumination. A correct interpretation of R_{sc} measurement or, in general, of collection in amorphous *p-i-n* solar cells must include the state of charge of the defects in the regions close to the doped zones and, probably, the effect of the diffusion current. This is the theme of Sec. IV.

IV. ANALYTICAL DESCRIPTION

A. Equilibrium

In thermodynamic equilibrium, i.e., in the dark and without external voltage, the regions near the *p-i* and *i-n* interfaces are non-neutral due to the Fermi level shifts in these regions. In Fig. 6, where the band diagram of a *p-i-n* structure is shown, we can see the different regions in the intrinsic layer. Assuming discrete transition levels for the dangling bonds and using the zero-temperature approximation, three regions within the intrinsic layer can be identified, which vary according to the position of the Fermi level:

(A) Interface region (PI): between $x=0$ and $x=x_p$, where x_p is the *i* layer position where E_f is on the dangling bond level E^+. All defects are positively ionized. The potential variation V_p across the PI region is determined by the difference between the Fermi level position in the *p*-doped material and the E^+ level of the dangling bond. The electric field strength decreases as a consequence of the defect charge:

$$E(x)=E_0-q\frac{N_{\mathrm{DB}}}{\varepsilon}x, \tag{22}$$

where the absolute value of the electric field is considered. E_0 is the field value at the interface *p-i* ($x=0$) and N_{DB} is the defect density.

(B) Bulk region (I): between $x=x_p$ and $x=x_n$, where x_n is the *i* layer position at which E_f is on the dangling bond level E^-. All defects are neutral and the voltage V_i across this region could be determined by the difference between the E^+ and E^- levels of the dangling bond, i.e., by the correlation energy U_{eff}. The electric field is uniform [$E(x)=E_i$].

(C) Interface region (IN): between $x=x_n$ and $x=L$. All defects are negatively ionized. The potential variation V_n across the IN region is determined by the difference between the Fermi level position in the n-doped material and the E^- level of the dangling bond. The electric field strength is

$$E(x)=E_L-q\frac{N_{\mathrm{DB}}}{\varepsilon}(L-x), \tag{23}$$

where E_L is the absolute value of the electric field at the interface *i-n* ($x=L$).

Thus, the electric field profile can be expressed in terms of five parameters: E_0, E_i, E_L, W_p and W_n; where W_p and W_n are the widths of the interface regions ($W_p=x_p$ and $W_n=L-x_n$). These parameters can be obtained as a function of the intrinsic layer thickness L and the potentials V_p, V_i, and V_n by solving the following set of equations:

$$(E_0+E_i)W_p=2V_p, \tag{24a}$$

$$(E_L+E_i)W_n=2V_n, \tag{24b}$$

$$E_i(L-W_p-W_n)=V_i, \tag{24c}$$

$$E_0-E_i=\frac{qN_{\mathrm{DB}}}{\varepsilon}W_p, \tag{24d}$$

$$E_L-E_i=\frac{qN_{\mathrm{DB}}}{\varepsilon}W_n, \tag{24e}$$

which is obtained by integrating the electric field profiles across the different regions of the *i* layer and imposing con-

Downloaded 15 Jun 2010 to 161.116.168.169. Redistribution subject to AIP license or copyright; see http://jap.aip.org/jap/copyright.jsp

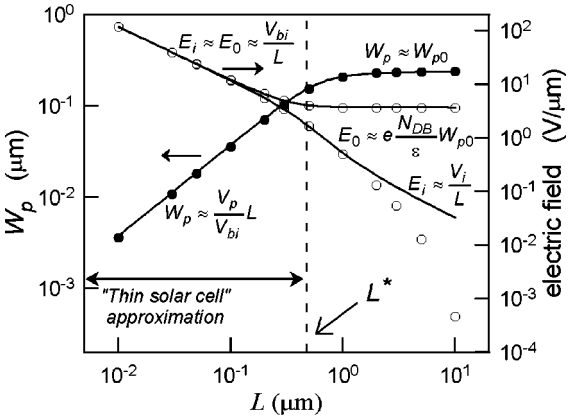

FIG. 7. Parameters of the electric field profile in equilibrium as a function of the *i* layer thickness L. Solid lines are theoretical results calculated from Eq. (24). Data points are from numerical simulation. Note that the cell described in Table I is symmetric so that $W_p = W_n$ and $E_0 = E_L$.

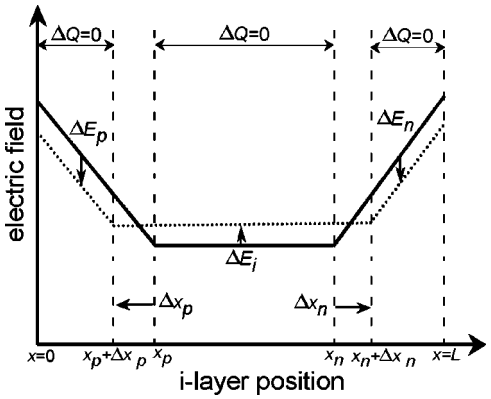

FIG. 8. Perturbation of electric field profile due to illumination.

tinuity of the electric field at the limits x_p and x_n. Note that the potential variations V_p, V_i, and V_n depend only on the doping level and the energetic position of the dangling bond in the intrinsic material, and the sum of these potentials is the built-in potential $V_{\rm bi}$ (i.e., the total potential variation across the *i* layer).

B. ''Thin solar cell'' approximation

The set of equations (24) can be solved easily by iterative methods (although it can also be solved analytically, the general solution is not straightforward). Figure 7 shows the dependence of the electric field profile (i.e., the parameters E_0, E_i, E_L, W_p, and W_n) on the intrinsic layer thickness L for the *p-i-n* solar cell described in Table I. We also compare the values obtained by solving the set of equations (24) with the values extracted from the numerical results. This plot gives two different kinds of behavior, depending on whether the *i* layer thickness L is bigger or smaller than a critical thickness value L^* related to the widths of the depletion layers in an ''infinite thick solar cell:''

$$L^* = W_{p0} + W_{n0}, \tag{25}$$

with

$$W_{p0} = \sqrt{\frac{2\varepsilon}{qN_{\rm DB}}V_p}$$

and (26)

$$W_{n0} = \sqrt{\frac{2\varepsilon}{qN_{\rm DB}}V_n}.$$

With the cell parameters listed in Table I we obtain $L^* \approx 0.5\mu$m. At the limit of thick cells (i.e., if $L \gg L^*$), the widths of the interface regions W_p and W_n tend to W_{p0} and W_{n0}, respectively. In this case, the electric field in the *i* layer departs significantly from uniformity ($E_i \ll E_0$ and $E_i \ll E_L$). In fact, the set of equations (24), where we use the zero-temperature approximation, leads to $E_i \approx V_i/L$, while numerical simulation shows that the electric field is much more sensitive to the *i* layer thickness and E_i is virtually zero. This is a consequence of the trapped charge in the interior of the *i* layer, near the PI and IN regions, due to the effect of the nonzero temperature.

However, this first study focuses on the most common situation of ''thin'' solar cells (i.e., when $L < L^*$). As can be seen in Fig. 7, in this case there is an important and nearly uniform electric field all over the *i* layer:

$$E_i \approx E_0 \approx E_L \approx \frac{V_{\rm bi}}{L}. \tag{27}$$

Note that, although in this situation the hypothesis of ''uniform field'' is a good assumption, the charged regions (PI and IN) in the *i* layer should not be neglected: the widths W_p and W_n are an important fraction of the *i* layer thickness. We find

$$W_p \approx \frac{V_p}{V_{\rm bi}}L$$

and (28)

$$W_n \approx \frac{V_n}{V_{\rm bi}}L.$$

C. Solar cell under uniform illumination

In general, when the solar cell is under external perturbation (illumination or electrical bias), the profile of charge density changes and, in consequence, the electric field profile also changes. The greatest variation in charge density occurs at the limits x_p and x_n of the interface regions. In the bulk of these regions the electric charge is mainly due to ionized defects and only a very high illumination level (or applied voltage) can perturb this ''fixed'' charge. Note that in the bulk of the neutral I region, between x_p and x_n, the effect of the photogenerated space charge could be more important. However we assume, as a first approach, that this effect is not significant. Therefore, we will interpret the perturbation of the charge profile as the variations Δx_p and Δx_n for the limits x_p and x_n of the interface regions (see Fig. 8). As a consequence of this perturbation, the electric field will be modified by the increments $\Delta E_p, \Delta E_i$ and ΔE_n in the three regions of the cell (note that if $\Delta Q = 0$ in the bulk, then ΔE

Downloaded 15 Jun 2010 to 161.116.168.169. Redistribution subject to AIP license or copyright; see http://jap.aip.org/jap/copyright.jsp

is constant). In the short-circuit condition the following relationships between these increments and the variations Δx_p and Δx_n can be found:

$$\Delta E_p = \Delta E_i + \frac{qN_{\mathrm{DB}}}{\varepsilon}\Delta x_p, \tag{29a}$$

$$\Delta E_n = \Delta E_i - \frac{qN_{\mathrm{DB}}}{\varepsilon}\Delta x_n, \tag{29b}$$

$$\Delta E_p(W_p+\Delta x_p)+\Delta E_i(W_i-\Delta x_p+\Delta x_n) + \Delta E_n(W_n-\Delta x_n)=0, \tag{29c}$$

where the first two equations in Eq. (29) are obtained by imposing continuity of the electric field at the new limits of the interface regions, and the last equation (29c) refers to the short-circuit condition: i.e., the integral of the electric field perturbation across the *i* layer must be zero.

We need two more equations to calculate the variation in the electric field profile ($\Delta E_p, \Delta E_i, \Delta E_n, \Delta x_p$, and Δx_n). These can be obtained employing statistics. For example: note that, in thermodynamic equilibrium and using the zero-temperature approach, the limit x_p was defined as the position in the *i* layer at which defects pass from the positive to the neutral state; i.e., $E_f(x_p)=E^+(x_p)$ (see Fig. 6). Equation (16a) shows that if $T\neq 0$, then at x_p the ratio T^+ for positive to neutral defects is 1/2. When the cell is under illumination, this condition will be accomplished at the new limit $x_p+\Delta x_p$. So, from the more general dangling-bond statistics [see Eqs. (15) and (16)], the following conditions at the new limits of the interface regions can be derived:

$$C^+\frac{p(x_p+\Delta x_p)-p_{\mathrm{eq}}(x_p)}{n(x_p+\Delta x_p)-n_{\mathrm{eq}}(x_p)} = C^-\frac{n(x_n+\Delta x_n)-n_{\mathrm{eq}}(x_n)}{p(x_n+\Delta x_n)-p_{\mathrm{eq}}(x_n)} = \frac{1}{2}, \tag{30}$$

where C^+ and C^- are the ratio of capture cross sections for charged to neutral defects: $C^+=\sigma_p^0/\sigma_n^+$ and $C^-=\sigma_n^0/\sigma_p^-$.

Now, in Eq. (30) we need to know the photogenerated carrier densities in order to solve the coupled set of Eqs. (29) and (30). Assuming that in the neutral region photocarrier transport occurs by field-assisted drift, and neglecting recombination in Eqs. (13a) and (13b) (see Ref. 5), then we arrive at

$$\Delta p(x)\approx\frac{G(L-x)}{\mu_p E(x)} \qquad \Delta n(x)\approx\frac{Gx}{\mu_n E(x)}. \tag{31}$$

As we discussed at the end of Sec. III, these expressions can be considered valid in the neutral region and valid only for minority carriers in the interface regions (electrons in the PI region and holes in the IN region). For the majority carriers diffusion cannot be ignored and the modified field has to be borne in mind on determining the drift. However, by solving the transport equations in the absence of recombination, simple expressions for the profiles of majority photocarriers are obtained (see Appendix A). So, for the PI region the result is that

$$\Delta p(x)\approx p_{\mathrm{eq}}(x)\left(e^{-(\Delta E_p x/V_T)}-1\right), \tag{32}$$

where V_T is the Boltzmann potential and $p_{\mathrm{eq}}(x)$ is the hole profile in equilibrium which can be calculated from the electric field profile in equilibrium, making $j_p(x)=0$ in Eq. (12a):

$$p_{\mathrm{eq}}(x)=p_{\mathrm{eq}}(0)\exp\left[-\frac{x}{V_T}\left(E_0-\frac{qN_{\mathrm{DB}}}{2\varepsilon}x\right)\right]. \tag{33}$$

Note that the illumination dependence in Eq. (32) is implicit in ΔE_p. For photoelectrons in the IN region we arrive at a similar expression, but in the function of ΔE_n. Now, using Eqs. (31) and (32) in Eq. (30) and solving the coupled set of equations (29)–(30), we can calculate the perturbation of the electric field profile due to illumination.

In the case of thin solar cells (i.e., when the ''thin solar cell'' approximation can be applied) a useful simplification is to assume that the electric field increments can be neglected in comparison with the electric field value E_i in the *i* layer. It can be shown that this simplification enables the effect of these increments in Eq. (32) to be removed. Thus, from Eq. (30), we arrive at the following expressions for the thickness variations Δx_p and Δx_n of the interface regions:

$$C^+ p_{\mathrm{eq}}(x_p)\left[\exp\left(-\frac{E_i\Delta x_p}{V_T}\right)-1\right]=\frac{G}{\mu_n E_i}(W_p+\Delta x_p), \tag{34a}$$

$$C^- n_{\mathrm{eq}}(x_n)\left[\exp\left(\frac{E_i\Delta x_n}{V_T}\right)-1\right]=\frac{G}{\mu_p E_i}(W_n-\Delta x_n), \tag{34b}$$

where $p_{\mathrm{eq}}(x_p)$ and $n_{\mathrm{eq}}(x_n)$ only depend on the position of the electronic defect states:

$$p_{\mathrm{eq}}(x_p)=p_{\mathrm{eq}}(0)\exp\left[-\frac{V_p}{V_T}\right]=N_V\exp\left[-\frac{E^+-E_V}{qV_T}\right], \tag{35a}$$

$$n_{\mathrm{eq}}(x_n)=n_{\mathrm{eq}}(L)\exp\left[-\frac{V_n}{V_T}\right]=N_C\exp\left[-\frac{E_C-E^-}{qV_T}\right]. \tag{35b}$$

The equations for Δx_p and Δx_n in Eq. (34) are transcendent and must be solved by iterative methods. However, for low perturbation we can assume that $|\Delta x_p|\ll W_p$ and $|\Delta x_n|\ll W_n$, and then we can obtain analytical solutions for Δx_p and Δx_n. For example, if Δx_p is neglected in the right term of Eq. (34a) then we arrive at

$$\Delta x_p=-\frac{V_T}{E_i}\ln\left(\frac{GW_p}{C^+ p_{\mathrm{eq}}(x_p)\mu_n E_i}+1\right). \tag{36}$$

This result shows that illumination leads to a decrease in the thickness of the interface region.

D. Voltage dependence of the electric field profile

In order to evaluate short-circuit resistance, it is necessary to calculate the derivatives of the field profile param-

Downloaded 15 Jun 2010 to 161.116.168.169. Redistribution subject to AIP license or copyright; see http://jap.aip.org/jap/copyright.jsp

eters with respect to the applied voltage. From the electric field profile under short-circuit conditions (i.e., E_0^*, E_i^*, E_L^*, W_p^*, and W_n^*, where the superscript * refers to the value under illumination: e.g., $W_p^* = W_p + \Delta x_p$), and following an analysis similar to the one made in the previous section (see Appendix B), we arrive at

$$\left(\frac{\delta E_i^*}{\delta V}\right)_{V=0} = \left(\frac{\delta E_0^*}{\delta V}\right)_{V=0} = \left(\frac{\delta E_L^*}{\delta V}\right)_{V=0} = -\frac{1}{L}, \tag{37a}$$

$$\left(\frac{\delta W_p^*}{\delta V}\right)_{V=0} = \frac{W_p^*}{V_{\rm bi}}, \tag{37b}$$

$$\left(\frac{\delta W_n^*}{\delta V}\right)_{V=0} = \frac{W_n^*}{V_{\rm bi}}; \tag{37c}$$

in which ''thin solar cell'' approximation is included.

E. Recombination and $\mu\tau$ product

Recombination in the *i* layer is due to dangling bonds and depends on their charge states in the different regions. Inside the *i* layer (I region) all defects can be considered as neutral and we can use the linear approximation of the recombination function [Eq. (1)]. In the interface PI region, where defects are positively ionized and electrons are minority carriers, the recombination rate is approximately

$$R^{pi} \approx \frac{\Delta n}{\tau_n^+} \tag{38}$$

with

$$\tau_n^+ = (v_{\rm th}\sigma_n^+ N_{\rm DB})^{-1},$$

where τ_n^+ is the capture time of free electrons by positively ionized dangling bonds and σ_n^+ is the corresponding capture cross section. The analogous equation for the recombination rate in the IN region is

$$R^{\rm in} \approx \frac{\Delta p}{\tau_p^-} \tag{39}$$

with

$$\tau_p^- = (v_{\rm th}\sigma_p^- N_{\rm DB})^{-1},$$

where τ_p^- is the capture time of free holes by negatively ionized dangling bonds and σ_p^- is the corresponding capture cross section.

To calculate the total recombination $I_{\rm rec}$ in the *i* layer, we must take into account the contribution of the different regions:

$$I_{\rm rec} = I_{\rm rec}^{pi} + I_{\rm rec}^{i} + I_{\rm rec}^{in} = \int_0^{x_p^*} \frac{\Delta n}{\tau_n^+} dx + \int_{x_p^*}^{x_n^*} \left(\frac{\Delta n}{\tau_n^0} + \frac{\Delta p}{\tau_p^0}\right) dx + \int_{x_n^*}^{L} \frac{\Delta p}{\tau_p^-} dx, \tag{40}$$

where, as mentioned earlier, Δn and Δp can be approximated by Eqs. (31) (note that recombination in the interface regions is dependent only on the minority-carrier densities).

Therefore, by solving the integrals in Eq. (40) we can obtain the recombination in the different regions. In the neutral region integration is straightforward and gives

$$I_{\rm rec}^{i} = \frac{1}{\mu\tau_{\rm eff}} \frac{(L - W_p^* - W_n^*)}{E_i^*} I_{\rm ph}, \tag{41}$$

where $\mu\tau_{\rm eff}$ is the same *effective* $\mu\tau$ product obtained by the standard uniform-field model of Hubin and Shah [i.e., see Eq. (8)). It is important to note that at the limit of very high illumination, W_p^* and W_n^* can be ignored in front of L, so that the same behavior as in the standard model is found [see Eq. (9)].

At low illumination and, in fact, in a wide range of intermediate illuminations, the widths of the interface regions are important and this means that recombination is determined by the charged defects (with higher capture cross sections than the neutral ones). Integrating Eq. (38) between the limits of the PI region, and using the ''thin solar cell'' approximation, we arrive at

$$I_{\rm rec}^{pi} = \frac{1}{\mu_n \tau_n^+} \frac{W_p^{*2}}{2LE_i^*} I_{\rm ph}. \tag{42}$$

In the IN region a similar expression can be obtained as a function of the width W_n^* and the $\mu\tau$ product for negatively ionized dangling bonds ($\mu_p\tau_p^-$). Finally, after some manipulation, we arrive at the following expression for the total recombination in the interface regions:

$$I_{\rm rec}^{pi+in} = I_{\rm rec}^{pi} + I_{\rm rec}^{in} = \frac{1}{\mu\tau_{\rm eff}^{pi+in}} \frac{L}{E_i^*} I_{\rm ph}, \tag{43}$$

where a new *effective* $\mu\tau$ product has been introduced:

$$\mu\tau_{\rm eff}^{pi+in} = 2\frac{\xi^+ \mu_n \tau_n^+ \xi^- \mu_p \tau_p^-}{\xi^+ \mu_n \tau_n^+ + \xi^- \mu_p \tau_p^-}. \tag{44}$$

The coefficients ξ^+ and ξ^- are dimensionless and depend on the ratio of the *i* layer thickness L to the interface widths:

$$\xi^+ = \left(\frac{L}{W_p^*}\right)^2$$

and

$$\xi^- = \left(\frac{L}{W_n^*}\right)^2. \tag{45}$$

Note that ξ^+ and ξ^+ depend strongly on illumination. For high illumination levels these coefficients greatly increase and for low illumination levels tend to a constant value which could be evaluated from Eq. (28) (for ''thin solar cells'').

Now, differentiating Eq. (43) with respect to the applied voltage [including the voltage dependence of E_i^*, W_p^* and W_n^*, from Eq. (37)], the short-circuit resistance can be deduced:

Downloaded 15 Jun 2010 to 161.116.168.169. Redistribution subject to AIP license or copyright; see http://jap.aip.org/jap/copyright.jsp

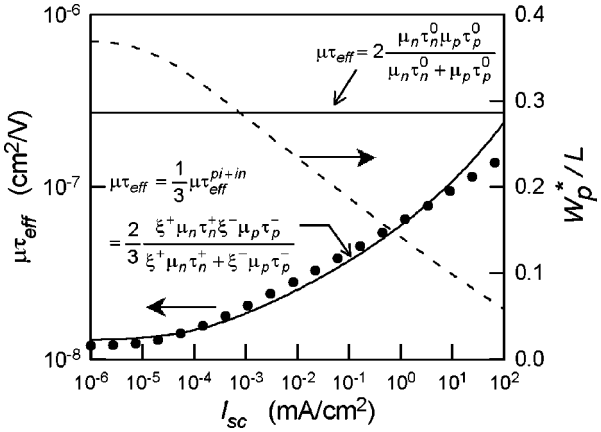

FIG. 9. $\mu\tau_{\text{eff}}$ as a function of I_{sc}. Solid lines are the theoretical values of $\mu\tau_{\text{eff}}$ for the I region and interfaces. Dashed line shows the illumination dependence of the width of the interface PI region deduced from Eq. (34). Data points are the values of $\mu\tau_{\text{eff}}$ deduced from numerical simulation of R_{sc}. ($L=0.3$ μm).

$$R_{\text{sc}} \approx \left(\frac{\delta I_{\text{rec}}^{pi+in}}{\delta V}\right)_{V=0}^{-1} = \frac{1}{3}\mu\tau_{\text{eff}}^{pi+in}E_i^{*2}I_{\text{ph}}^{-1} = \frac{1}{3}\mu\tau_{\text{eff}}^{pi+in}\left(\frac{V_{\text{bi}}}{L}\right)^2 I_{\text{ph}}^{-1}. \tag{46}$$

This expression is similar in form to the expression normally deduced from the uniform-field model [Eq. (10)] and, consequently, enables the same method to be used to analyze the variable irradiance measurement of R_{sc}. However, note that the interpretation of the $\mu\tau$ product can be very different.

Figure 9 compares the numerical and analytical $\mu\tau$ product calculations as a function of the short-circuit current I_{sc} for the 0.3-μm-thick solar cell with the set of parameters given in Table I. The numerical $\mu\tau$ product is deduced from the simulated short-circuit resistance R_{sc} as in Fig. 2. The analytical $\mu\tau$ product is separated into its two components: the bulk contribution, i.e., the standard effective $\mu\tau$ product given by Eq. (8) and the interface contribution given by Eq. (44) (to calculate the illumination dependence of the coefficients ξ^+ and ξ^- in Eq. (44), we employed the most accurate relationships given by Eq. (34)). Note that the total $\mu\tau$ product must be determined by the smaller of the two contributions and, as we can see in Fig. 9, this is precisely the interface contribution.

F. Influence of surface recombination

Until now we have assumed that the contacts $x=0$ and $x=L$, which define the limits of the i layer, are perfectly blocking for minority carriers: i.e., $S_L=0$ and $S_0=0$ in Eq. (21). However, minority carriers at the contacts are usually lost by surface recombination, and a current of the opposite sign to the active photocurrent forms. Now we examine the effect of this surface recombination on cells illuminated by uniformly absorbed light under short-circuit conditions. We focus on developing analytical expressions for the current loss at the interfaces and its dependence on voltage bias (i.e., short-circuit resistance).

Under short-circuit conditions, the photocurrent can be obtained by subtracting the different recombination currents from the photogeneration current in the i-layer I_{ph}:

$$I(V=0) = I_{\text{ph}} - I_{\text{rec}} - I_{\text{rec}}^s, \tag{47}$$

where I_{rec} is the bulk recombination current, which has been discussed already, and I_{rec}^s is the surface recombination, which can be expressed by the sum of the electron current at the p-i interface ($x=0$) and the hole current at the n-i interface ($x=L$):

$$I_{\text{rec}}^s = j_n(x=0) + j_p(x=L). \tag{48}$$

The most simple treatment is to assume that these minority currents are related to the excess of minority carriers at the interfaces according to

$$j_n(x=0) = qS_0\Delta n(0), \tag{49a}$$

$$j_p(x=L) = qS_L\Delta p(L), \tag{49b}$$

where the interface recombination velocities S_0 and S_L can be considered as constants.

Thus, in order to evaluate I_{rec}^s we need to calculate $\Delta n(0)$ and $\Delta p(L)$, which can be done by solving the transport equations in the regions near the interfaces. For this purpose it is useful to make some simplifying assumptions, the most obvious of which are that bulk recombination is negligible and the electric field is a constant. So, for instance, the electron photocurrent near the p-i interface ($x=0$) can be given by

$$j_n(x) = -q\mu_n\Delta n(x)E_0 + qV_T\mu_n\frac{d\Delta n(x)}{dx}, \tag{50}$$

where E_0 is the absolute value of the electric field. It is important to note that, despite the focus on the transport of minority carriers, the diffusion current is not ignored in Eq. (50). In fact, however strong the electric field E_0 may be, the assumption of photocarrier transport by field assistance is not correct in a narrow region close to the contact $x=0$ [note that, if $x=0$ in Eq. (50) this assumption leads to $S_0 = -\mu_nE_0$, which is incoherent]. In the remaining portion of the PI region the field-assisted transport approach is valid and so this assumption can properly be a boundary condition of our problem: as we move away from the contact, diffusion becomes negligible and the minority-carrier density can be given by Eq. (31).

Thus, using the most general expression, Eq. (50) in the continuity equation for photoelectrons, we arrive at the following differential equation:

$$\frac{d^2\Delta n}{dx^2} - \frac{E_0}{V_T}\frac{d\Delta n}{dx} = -\frac{G}{\mu_nV_T}. \tag{51}$$

This equation can be readily integrated, using the boundary condition that $\Delta n(x) = Gx/\mu_nE_0$ at ''$x\to\infty$,'' to give

$$\Delta n(x) = \Delta n(0) + \frac{Gx}{\mu_nE_0}. \tag{52}$$

Downloaded 15 Jun 2010 to 161.116.168.169. Redistribution subject to AIP license or copyright; see http://jap.aip.org/jap/copyright.jsp

This expression for $\Delta n(x)$ can be used in Eq. (50) to determine the electron photocurrent. Then, we can evaluate the electron photocurrent at $x=0$ and, eliminating $\Delta n(0)$ by means of Eq. (49a), we arrive at

$$j_n(0)=\frac{V_T}{E_0}\frac{S_0}{(S_0+\mu_n E_0)}G. \tag{53}$$

For the hole photocurrent at $x=L$ we can find a similar equation but expressed in terms of S_L, μ_p, and the absolute value E_L of the electric field near $x=L$. Now, differentiating Eq. (53) with respect to the applied voltage, we can deduce the contribution of the surface recombination at $x=0$ to the short-circuit resistance. There are two important limiting situations (we include the ''thin solar cell'' approximation, i.e., $E_0 \approx E_i \approx V_{\rm bi}/L$):

(A) Weak surface recombination ($S_0 \ll \mu_n E_i$):

$$I^s_{\rm rec}=\frac{V_T}{V_{\rm bi}^2}\frac{S_0}{\mu_n}LI_{\rm ph}, \tag{54a}$$

$$R_{\rm sc}=\frac{V_{\rm bi}^3}{2V_T}\frac{\mu_n}{S_0}L^{-1}I_{\rm ph}^{-1}. \tag{54b}$$

(B) Strong surface recombination ($S_0 \gg \mu_n E_i$):

$$I^s_{\rm rec}=\frac{V_T}{V_{\rm bi}}I_{\rm ph}, \tag{55a}$$

$$R_{\rm sc}=\frac{V_{\rm bi}^2}{V_T}I_{\rm ph}^{-1}. \tag{55b}$$

A significant aspect of these results is the dependence of $R_{\rm sc}$ on the *i* layer thickness L: for weak surface recombination, $R_{\rm sc}$ is proportional to L^{-1} and, for strong surface recombination, $R_{\rm sc}$ is independent of L. This behavior is different from what is found in the case of bulk recombination, in which $R_{\rm sc}$, derived from the voltage dependence of recombination in both neutral and interface regions, is proportional to L^{-2}.

In order to examine the effect of the surface recombination , and to check the validity of Eqs. (54) and (55), Fig. 10 shows plots of the numerical and analytical $R_{\rm sc}$ calculations as a function of S_0 for solar cells with different *i*-layer thickness (the remaining cell parameters are given in Table I). We consider uniform illumination with $I_{\rm ph}=10^{-3}$ mA/cm^2. Figure 10 shows that $R_{\rm sc}$ is only determined by surface recombination in the case of very thin solar cells ($L<0.3\mu$m), and at sufficiently high S_0 ($>10^4$ cm/s).

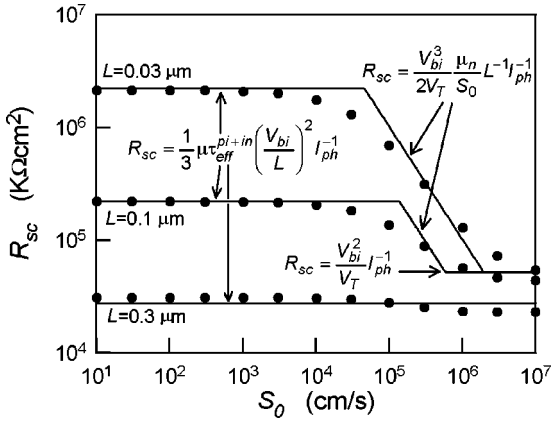

FIG. 10. Short-circuit resistance as a function of the surface recombination rate S_0 for solar cells with different *i* layer thickness. It is considered that $I_{\rm ph}=10^{-3}$ mA/cm^2. Solid lines are the theoretical values of $R_{\rm sc}$ (the main contribution is plotted) and data points are the values of $R_{\rm sc}$ obtained from numerical simulation. (We assume that the contact $x=L$ is perfectly blocking.)

V. SUMMARY

Our numerical simulation results reproduce the experimental data of the illumination dependence of the short-circuit resistance $R_{\rm sc}$ in *a*-Si:H *p-i-n* solar cells. These results suggest that recombination in the charged regions of the *i* layer should not be overlooked. We then developed a new analytical model to describe collection in *p-i-n* structures under short-circuit conditions and uniform illumination. The recombination current and the short-circuit resistance can be given as a function of a $\mu\tau$ product which adequately combines two effective $\mu\tau$ products for the different regions in the *i* layer: (1) for the neutral region in the bulk of the *i* layer we find the same effective $\mu\tau$ product as is obtained with the standard uniform-field model, (2) for the charged regions at the interfaces we find a new *effective* $\mu\tau$ product which is light-dependent. We show that recombination and $R_{\rm sc}$ are determined by this latter $\mu\tau$ product in a wide range of illumination.

We also examined the effect of surface recombination. We demonstrated that, under uniform illumination and short-circuit conditions, surface recombination could not be negligible in very thin solar cells at sufficiently high surface recombination rates. It could be evaluated by a check on the effect of the *i*-layer thickness on $R_{\rm sc}$.

We have also shown that, in the analysis of *p-i-n* solar cells, it is necessary to take into consideration both the diffusion process for majority carriers at interfaces and the effect of the variation in the electric field. We obtained elementary expressions that can be used in analyzing the general behavior of *p-i-n* solar cells.

ACKNOWLEDGMENTS

The authors thank Professor A. V. Shah for valuable discussions. This study was supported by the CRYSTAL program of the EC (Grant No. JOR3-CT97-0126).

APPENDIX A: MAJORITY-CARRIER PROFILES IN SHORT-CIRCUIT CONDITIONS

In the interface regions near the doped layers, the majority-carrier densities and the gradients are important: carrier diffusion from the doped regions cannot be ignored in determining the transport and. moreover, the electric field variation ΔE caused by illumination can also contribute to the photocurrent. Thus, in the PI region the hole photocurrent, expressed in terms of increments, should be given by

Downloaded 15 Jun 2010 to 161.116.168.169. Redistribution subject to AIP license or copyright; see http://jap.aip.org/jap/copyright.jsp

$$j_p(x)/q = -\mu_p p_{eq}(x)\Delta E_p - \mu_p[E_{eq}(x)+\Delta E_p]\Delta p(x) - \mu_p V_T \frac{d\Delta p}{dx}, \tag{A1}$$

where $p_{eq}(x)$ is the hole density profile in equilibrium [given by Eq. (33)], $E_{eq}(x)$ is the electric field profile in equilibrium [note that it is positive, see Eq. (22)], and ΔE_p is the electric field variation in the PI region due to illumination. As has been discussed, the photogenerated space charge in the bulk of the PI region is negligible, and so it can be assumed that ΔE_p is a constant. Thus, introducing Eq. (A1) into the continuity equation, and ignoring recombination, we find the following differential equation for the hole density increment in the PI region:

$$\frac{d^2\Delta p}{dx^2} + \frac{1}{V_T}[E_{eq}(x)+\Delta E_p]\frac{d\Delta p}{dx} - \frac{1}{V_T}\frac{qN_{DB}}{\varepsilon}\Delta p = -\frac{G}{V_T\mu_p} - \frac{\Delta E_p}{V_T}\frac{dp_{eq}}{dx}. \tag{A2}$$

This equation can be solved for Δp and gives a relatively complicated expression which is expressed in terms of the error function Erf(y). It can be demonstrated that this function is well approximated by $1-e^{-y^2}/\sqrt{\pi}y$ and, using the boundary condition that $\Delta p(x=0)=0$ (i.e., assuming ohmic contact), after some manipulation we arrive at

$$\Delta p(x) = p_{eq}(x)\left[(1-C)\exp\left(-\frac{\Delta E_p x}{V_T}\right)-1\right] + \frac{\mu_p p_{eq}(0)(E_0+\Delta E_p)C - Gx}{\mu_p[E_{eq}(x)+\Delta E_p]}, \tag{A3}$$

where C is the constant of integration that we should obtain by imposing a new condition. To this effect, from Eq. (A3) we can calculate the hole photocurrent in the PI region. It can be demonstrated that only the drift component of the second term on the right-hand side of Eq. (A3) significantly contributes to the photocurrent (the first term gives a diffusion component that is compensated by drift). The result is that

$$j_p(x)/q \approx Gx - \mu_p p_{eq}(0)(E_0+\Delta E_p)C. \tag{A4}$$

On the other hand, from the continuity equation for holes, neglecting recombination and imposing $j_p(L)=0$, we find

$$j_p(x)/q = -G(x-L), \tag{A5}$$

then, equating Eqs. (A4) and (A5) we can determine the value of C:

$$C = \frac{GL}{\mu_p p_{eq}(0)(E_0+\Delta E_p)}. \tag{A6}$$

For a typical solar cell (defined by the set of parameters given in Table I) under high illumination ($I_{ph}=10$ mA/cm^2) we find $C\approx 10^{-4}$, so that $C \ll 1$, and so this constant can be safely ignored in the first term of Eq. (A3). Finally, substitution of Eq. (A6) into Eq. (A3) yields

$$\Delta p(x) = p_{eq}(x)\left[\exp\left(-\frac{\Delta E_p x}{V_T}\right)-1\right] + \frac{G}{\mu_p(E_{eq}(x)+\Delta E_p)}(L-x) \tag{A7}$$

Note that the second term in Eq. (A7) is the photogenerated hole distribution that we obtain making the field-assisted drift assumption [see Eq. (31)] and, as we have seen from Fig. 5, this is only a very small fraction of the total. We thus obtain the relationship given by Eq. (32) for the photogenerated hole profile in the PI region.

APPENDIX B: EFFECT OF APPLIED VOLTAGE (DERIVATIVES)

We examined a *p-i-n* solar cell in short-circuit conditions under weakly absorbed light. Illumination alters the electric field profile by the increments $\Delta x_p, \Delta x_n, \Delta E_p, \Delta E_i$, and ΔE_n, so that the analytical expressions for the profiles of electric field and carrier densities are:

(A) PI region ($0<x<W_p^*$):

$$E^*(x) = E_0^* - \frac{qN_{DB}}{\varepsilon}x, \tag{B1a}$$

$$p^*(x) \approx p_{eq}(0)\exp\left[-\frac{x}{V_T}\left(E_0^* - \frac{qN_{DB}}{2\varepsilon}x\right)\right], \tag{B1b}$$

$$n^*(x) \approx \frac{Gx}{\mu_n E^*(x)}. \tag{B1c}$$

(B) I region ($W_p^*<x<W_n^*$):

$$E^*(x) = E_i^*, \tag{B2a}$$

$$p^*(x) \approx \frac{G(L-x)}{\mu_p E_i^*}, \tag{B2b}$$

$$n^*(x) \approx \frac{Gx}{\mu_n E_i^*}. \tag{B2c}$$

(C) IN region ($W_n^*<x<L$):

$$E^*(x) = E_L^* - \frac{qN_{DB}}{\varepsilon}(L-x), \tag{B3a}$$

$$p^*(x) \approx \frac{G(L-x)}{\mu_p E^*(x)}, \tag{B3b}$$

$$n^*(x) \approx n_{eq}(L)\exp\left[-\frac{(L-x)}{V_T}\left(E_L^* - \frac{qN_{DB}}{2\varepsilon}(L-x)\right)\right]. \tag{B3c}$$

The superscript * in Eqs. (B1)–(B3) refers to the value under illumination. In this situation, if a small external voltage V is applied, then the electric profile will change. The widths W_p^* and W_n^* will be modified by the new increments Δx_p^v and Δx_n^v, respectively, and, assuming that the variation of the space charge in the bulk of the different regions is negligible, the electric field will be modified by the constants ΔE_p^v,

Downloaded 15 Jun 2010 to 161.116.168.169. Redistribution subject to AIP license or copyright; see http://jap.aip.org/jap/copyright.jsp

ΔE_i^v, and ΔE_n^v. Using an argument similar to the one in Sec. III C, we find the following relationship among these increments:

$$\Delta E_p^v = \Delta E_i^v + \frac{qN_{\mathrm{DB}}}{\varepsilon}\Delta x_p^v, \tag{B4a}$$

$$\Delta E_n^v = \Delta E_i^v - \frac{qN_{\mathrm{DB}}}{\varepsilon}\Delta x_n^v, \tag{B4b}$$

$$\Delta E_p^v W_p^* + \Delta E_i^v W_i^* + \Delta E_n^v W_n^* = -V; \tag{B4c}$$

where, in the last equation (B4c), we assume that the applied voltage is sufficiently small for $|\Delta x_p^v| \ll W_p^*$ and $|\Delta x_n^v| \ll W_n^*$. The two remaining equations can be obtained, as in Sec. III C, by imposing $T^+(x_p^* + \Delta x_p^v) = 1/2$ and $T^-(x_n^* + \Delta x_n^v) = 1/2$ [i.e., Eq. (30)].

On the other hand, if low applied voltage is assumed, it can be demonstrated that the most significant perturbation of carrier distribution occurs for majority carriers in the interface regions. To obtain the hole profile in the PI region, we can reach a differential equation similar to Eq. (A2) but for the hole density increment due to the electrical bias. Thus, solving the differential equation, we find that the total hole density in the PI region is well approximated by

$$p(x) \approx p^*(x)\exp\left[-\frac{\Delta E_p^v}{V_T}x\right], \tag{B5}$$

where $p^*(x)$ is the hole distribution in the PI region for the cell in short-circuit conditions under illumination. Now, introducing Eq. (B5) in the condition $T^+(x_p^* + \Delta x_p^v) = 1/2$ we arrive at

$$p^*(x_p^*)\exp\left[-\frac{1}{V_T}(E_i^*\Delta x_p^v + x_p^*\Delta E_p^v)\right] \approx \frac{GW_p^*}{\mu_n E_i^* C^+} + p_{\mathrm{eq}}(x_p), \tag{B6}$$

where the second term could be considered a constant. So, differentiating Eq. (B6) with respect to V we obtain

$$\frac{d\Delta x_p^v}{dV} = -\frac{W_p^*}{E_i^*}\frac{d\Delta E_p^v}{dV}. \tag{B7}$$

From this equation and differentiating Eq. (B4a), we arrive at the following relationship between the derivatives of E_p^* and E_i^*:

$$\left(\frac{\delta E_p^*}{\delta V}\right)_{V=0} = \frac{E_i^*}{E_0^*}\left(\frac{\delta E_i^*}{\delta V}\right)_{V=0}. \tag{B8}$$

Using similar reasoning in the IN region, we could arrive at

$$\left(\frac{\delta E_n^*}{\delta V}\right)_{V=0} = \frac{E_i^*}{E_L^*}\left(\frac{\delta E_i^*}{\delta V}\right)_{V=0}. \tag{B9}$$

It now remains to calculate the derivative of E_i^* with respect to V. This can be done by differentiating Eq. (B4c) and using Eqs. (B8) and (B9). We find

$$\left(\frac{\delta E_i^*}{\delta V}\right)_{V=0} = -\left(\frac{E_i^*}{E_0^*}W_p^* + W_i^* + \frac{E_i^*}{E_L^*}W_n^*\right)^{-1}. \tag{B10}$$

For ''thin'' solar cells, it can be shown that this last derivative reduces to $-1/L$. Also, for high illumination levels, when the neutral I region fills the *i* layer, the derivative of E_i^* tends to $-1/L$.

Other useful relationships are the derivatives of W_p^* and W_n^* with respect to V. These can be most easily expressed as a function of the derivative of E_i^*

$$\left(\frac{\delta W_p^*}{\delta V}\right)_{V=0} = -\frac{W_p^*}{E_0^*}\left(\frac{\delta E_i^*}{\delta V}\right)_{V=0}, \tag{B11a}$$

$$\left(\frac{\delta W_n^*}{\delta V}\right)_{V=0} = -\frac{W_n^*}{E_L^*}\left(\frac{\delta E_i^*}{\delta V}\right)_{V=0}. \tag{B11b}$$

[1] M. Hack and M. Shur, J. Appl. Phys. **58**, 997 (1985).
[2] J. L. Gray, IEEE Trans. Electron Devices **ED-36**, 906 (1989).
[3] J. M. Asensi, J. Andreu, J. Puigdollers, J. Bertomeu, and J. C. Delgado, Mater. Res. Soc. Symp. Proc. **297**, 315 (1993).
[4] R. S. Crandall, J. Appl. Phys. **54**, 7176 (1983).
[5] J. Hubin and A. V. Shah, Philos. Mag. B **72**, 589 (1995).
[6] J. Merten, J. M. Asensi, C. Voz, A. V. Shah, R. Platz, and J. Andreu, IEEE Trans. Electron Devices **ED-45**, 423 (1998).
[7] S. S. Hegedus, Prog. Photovolt. Res. Appl. **5**, 151 (1997).
[8] J. Hubin, A. V. Shah, and E. Auvain, Philos. Mag. Lett. **66**, 115 (1992).
[9] A. V. Shah, J. Hubin, E. Sauvain, P. Pipoz, N. Beck, and N. Wyrsch, J. Non-Cryst. Solids **164–166**, 485 (1993).

Downloaded 15 Jun 2010 to 161.116.168.169. Redistribution subject to AIP license or copyright; see http://jap.aip.org/jap/copyright.jsp